

Carbon isotope fractionation during catabolism and anabolism in acetogenic bacteria growing on different substrates

- Supplementary

Christoph Freude, Martin Blaser

Department of Biogeochemistry, Max-Planck-Institute for Terrestrial Microbiology, Karl-von-Frisch-Str. 10, 35043 Marburg, Germany

Keywords: acetogen, homoacetogen, chemolithotroph, acetate.

Corresponding author:

Martin B. Blaser

Max Planck Institute for Terrestrial Microbiology

Karl-von-Frisch-Str. 10,

35043 Marburg, Germany

Tel: +49-6421-178 870

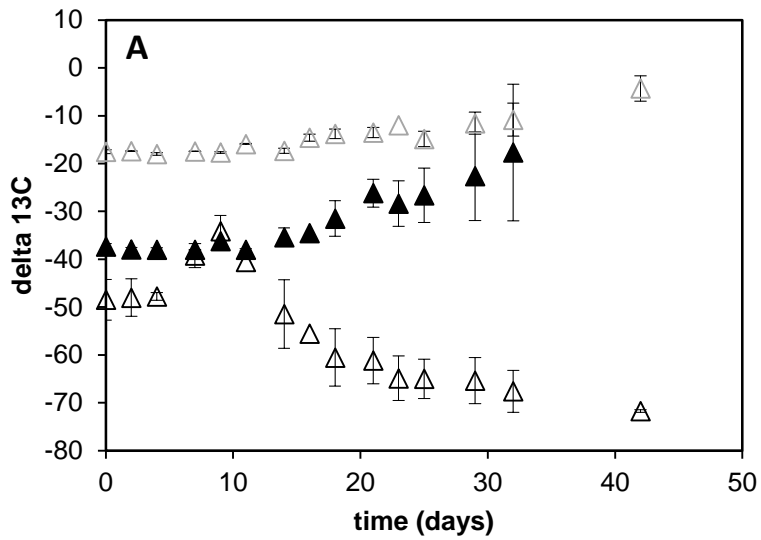
Fax: +49-6421-178 999

Email: blaserm@mpi-marburg.mpg.de

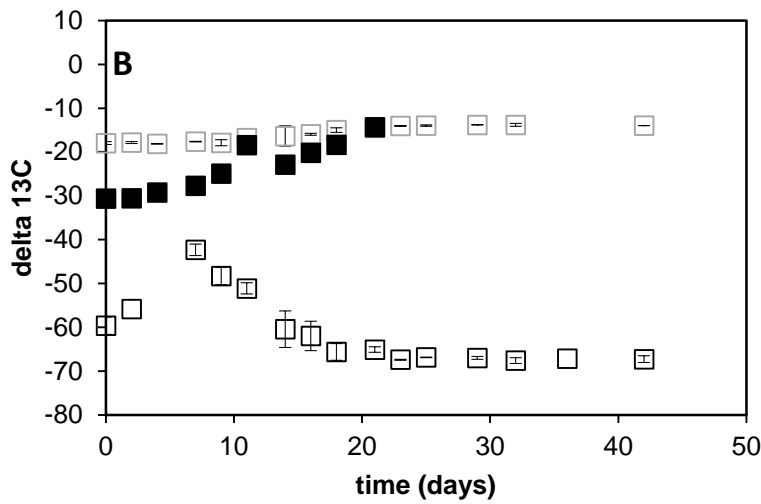
Table S1 Fractionation into biomass for different organisms

Organism	metabolism	substrate	temp	$\delta_{\text{substrate}}$	δ_{biomass}	$\Delta_{\text{substrate-biomass}}$	Reference
<i>Acetobacterium woodii</i>	acetogen	CO ₂	28	-49.5	-76.3	-26.8	Preuss et al. 1989
<i>Acetobacterium woodii</i>	acetogen	CO ₂	28	-49.8	-70.4	-20.6	Preuss et al. 1989
<i>Acetobacterim carbinolicum</i>	acetogen	CO ₂	37	-9.7	-26.8	-17.1	unpublished *
<i>Acetonea longum</i>	acetogen	CO ₂	37	-10.1	-25.7	-15.6	unpublished *
<i>Acetobacterium woodii</i>	acetogen	CO ₂	28	-47.6	-62.4	-14.8	Preuss et al 1989
<i>Thermoanaerobacter kivui</i>	acetogen	CO ₂	55	-13.3	-27.9	-14.6	unpublished *
<i>Thermoanaerobacter kivui</i>	acetogen	CO ₂	55	-13.5	-26.9	-13.4	unpublished *
<i>Moorella theromautotrophicum DSM 1974</i>	acetogen	CO ₂	55	-13.4	-26.3	-12.9	unpublished *
<i>Clostridium magnum</i>	acetogen	CO ₂	37	-10.0	-22.7	-12.7	unpublished *
<i>Clostridium acetium</i>	acetogen	CO ₂	37	-9.5	-21.7	-12.2	unpublished *
<i>Acetitomaaculum ruminis</i>	acetogen	CO ₂	37	-10.0	-20.8	-10.8	unpublished *
<i>Moorella thermoacetica DSM 2955</i>	acetogen	CO ₂	55	-10.3	-20.0	-9.7	unpublished *
<i>Sporomusa ovata</i>	acetogen	CO ₂	37	-11.2	-20.9	-9.7	unpublished *
<i>Moorella thermoacetica DSM 2955</i>	acetogen	CO ₂	55	-12.9	-22.2	-9.3	unpublished *
<i>Moorella thermoacetica DSM 2955</i>	acetogen	CO ₂	55	-12.8	-21.7	-8.9	unpublished *
<i>Acetobacterium woodii</i>	acetogen	CO ₂	37	-11.8	-20.5	-8.7	unpublished *
<i>Thermoanaerobacter kivui</i>	acetogen	CO ₂	55	-10.7	-18.8	-8.1	unpublished *
<i>Moorella theromautotrophicum DSM 1974</i>	acetogen	CO ₂	55	-12.9	-19.2	-6.3	unpublished *
<i>Thermoanaerobacter kivui</i>	acetogen	glucose	55	-13.1	-21.5	-8.4	unpublished *
<i>Thermoanaerobacter kivui</i>	acetogen	glucose	55	-13.4	-18.7	-5.3	compare Fig. S4A
<i>Thermoanaerobacter kivui</i>	acetogen	glucose	55	-12.8	-15.2	-2.4	unpublished *
<i>Moorella thermoacetica DSM 2955</i>	acetogen	glucose	55	-13.4	-15.6	-2.2	unpublished *
<i>Thermoanaerobacter kivui</i>	acetogen	glucose	55	-26.2	-26.9	-0.8	unpublished *
<i>Thermoanaerobacter kivui</i>	acetogen	glucose	55	-13.0	-13.5	-0.5	unpublished *
<i>Rhodococcus</i>	fermentation	glucose				-2.3	Zyakun et al. 2013
<i>E.coli</i>	fermentation	glucose		-10.2	-11.9	-1.7	Zhang et al. 2002
<i>Pseudomonas aureofaciens</i>	fermentation	glucose				-1.0	Zyakun et al. 2013
<i>E.coli</i>	fermentation	glucose		-9.0	-9.6	-0.6	Zhang et al. 2002
<i>E.coli</i>	fermentation	glucose		-10.0	-9.7	0.3	Zhang et al. 2002
<i>Pseudomonas aeruginosa</i>	fermentation	glucose		-13.3	-10.3	3.0	Zhang et al. 2002
<i>Methanosarcina barkeri</i>	methanogen	acetate	37	-30.9	-38.2	-7.3	Londry et al. 2008
<i>Methanosarcina barkeri</i>	methanogen	acetate	37	-30.9	-31.4	-0.5	Londry et al. 2008
<i>Methanosarcina barkeri</i>	methanogen	acetate	37	-25.3	-19.1	6.2	Goevert et al. 2009
<i>Methanosarcina acetivorans</i>	methanogen	acetate	37	-25.6	-18.5	7.1	Goevert et al. 2009
<i>M. lithoautotrophicus</i>	methanogen	CO ₂	65	-23.2	-51.2	-28.0	House et al. 2003
<i>M. lithoautotrophicus</i>	methanogen	CO ₂	65	-21.5	-49.1	-27.6	House et al. 2003
<i>M. lithoautotrophicus</i>	methanogen	CO ₂	65	-23.3	-50.2	-26.9	House et al. 2003
<i>M. lithoautotrophicus</i>	methanogen	CO ₂	65	-23.4	-49.4	-26.0	House et al. 2003
<i>M. lithoautotrophicus</i>	methanogen	CO ₂	70	-23.7	-49.4	-25.7	House et al. 2003
<i>Methanosarcina barkeri</i>	methanogen	CO ₂	37	-20.5	-44.5	-24.0	House et al. 2003
<i>M. lithoautotrophicus</i>	methanogen	CO ₂	65	-23.9	-47.6	-23.7	House et al. 2003
<i>M. thermoautotrophicus</i>	methanogen	CO ₂	45	-23.7	-46.4	-22.7	House et al. 2003
<i>M. lithoautotrophicus</i>	methanogen	CO ₂	60	-22.7	-44.9	-22.2	House et al. 2003
<i>M. thermoautotrophicus</i>	methanogen	CO ₂	65	-24.7	-46.7	-22.0	House et al. 2003
<i>M. janaschii</i>	methanogen	CO ₂	85	-26.0	-43.6	-17.6	House et al. 2003
<i>M. thermoautotrophicus</i>	methanogen	CO ₂	45	-21.9	-39.1	-17.2	House et al. 2003
<i>Methanobacterium thermoautotrophicus</i>	methanogen	CO ₂	65	-23.2	-40.2	-17.0	House et al. 2003
<i>M. lithoautotrophicus</i>	methanogen	CO ₂	51	-22.1	-38.9	-16.8	House et al. 2003
<i>Methanosarcina barkeri</i>	methanogen	CO ₂	37	-28.5	-44.1	-15.6	Londry et al. 2008
<i>M. janaschii</i>	methanogen	CO ₂	85	-25.0	-39.6	-14.6	House et al. 2003
<i>Methanosarcina barkeri</i>	methanogen	CO ₂	37	-31.2	-45.1	-13.9	Londry et al. 2008
<i>Methanopyrus kandleri</i>	methanogen	CO ₂	100	-24.3	-37.4	-13.1	House et al. 2003
<i>M. janaschii</i>	methanogen	CO ₂	85	-24.8	-36.7	-11.9	House et al. 2003
<i>M. lithoautotrophicus</i>	methanogen	CO ₂	41	-21.9	-33.3	-11.4	House et al. 2003
<i>M. thermoautotrophicus</i>	methanogen	CO ₂	65	-23.1	-34.4	-11.3	House et al. 2003
<i>M. thermoautotrophicus</i>	methanogen	CO ₂	45	-21.9	-30.8	-8.9	House et al. 2003
<i>M. janaschii</i>	methanogen	CO ₂	85	-23.5	-31.3	-7.8	House et al. 2003
<i>Methanosarcina barkeri</i>	methanogen	methanol	37	-46.2	-77.3	-31.1	Londry et al. 2008
<i>Methanobolus zinderi</i>	methanogen	methanol	37	-38.6	-62.4	-23.8	Penger et al. 2013
<i>Methanosarcina acetivorans</i>	methanogen	methanol	37	-39.0	-62.8	-23.8	Penger et al. 2013
<i>Methanosarcina barkeri</i>	methanogen	methanol	37	-38.4	-62.1	-23.7	Penger et al. 2013
<i>Methanosarcina barkeri</i>	methanogen	methanol	37	-46.2	-46.1	0.1	Londry et al. 2008
<i>Ectothiorhodospira shaposhnikovii</i>	phototroph	CO ₂				-15.0 to -34.3	Zyakun et al. 2009
<i>Lamprocystis purpureus</i>	phototroph	CO ₂				-10.4 to -31.9	Zyakun et al. 2009
<i>Thiocapsa sp.</i>	phototroph	CO ₂				-21.9 to -29.1	Zyakun et al. 2009
<i>Prosthecochloris sp.</i>	phototroph	CO ₂				-18.3 to -22.7	Zyakun et al. 2009
<i>Desulfobacter hydrogenophilus</i>	sulfate reducer	acetate	30	-25.3	-32.7	-7.4	Goevert et al. 2008
<i>Desulfobacter postgatei</i>	sulfate reducer	acetate	30	-25.6	-31.2	-5.6	Goevert et al. 2008
<i>Desulfobacterium autotrophicum</i>	sulfate reducer	CO ₂	28	-49.5	-85.4	-35.9	Preuss et al. 1989
<i>Desulfobacterium autotrophicum</i>	sulfate reducer	CO ₂	28	-49.8	-84.8	-35.0	Preuss et al. 1989
<i>Desulfobacter hydrogenophilus</i>	sulfate reducer	CO ₂	28	-47.6	-60.9	-13.3	Preuss et al. 1989
<i>Desulfobacter hydrogenophilus</i>	sulfate reducer	CO ₂	28	-49.8	-59.2	-9.4	Preuss et al. 1989
<i>Desulfobacter hydrogenophilus</i>	sulfate reducer	CO ₂	28	-49.5	-57.9	-8.4	Preuss et al. 1989

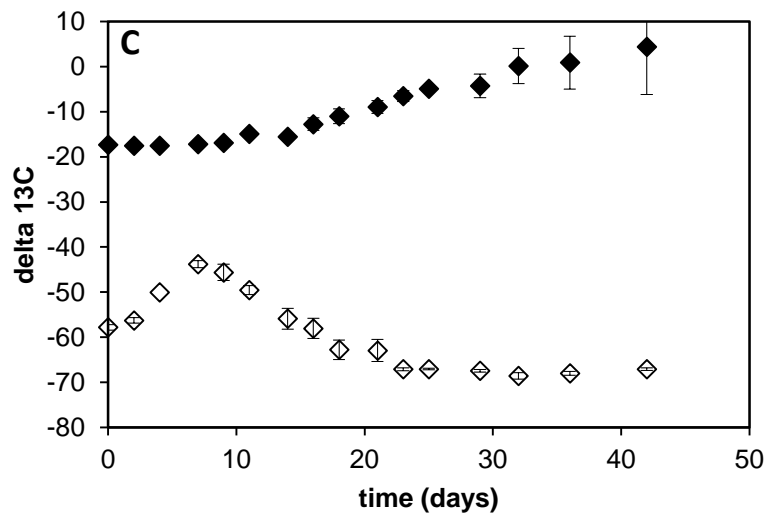
unpublished *: Most of the data shown for acetogenic pure cultures shown here originates from a study published in Blaser et al. Appl. Environ. Microbiol. (2013). In general the growth conditions were similar to the ones described in the Material and Methods section of current publication. Multiple entries for a given strain are for replicated incubations of the given strain.



△ CO2 (methanol) △ acetate (methanol) ▲ methanol (methanol)



□ CO2 (formate) □ acetate (formate) ■ formate (formate)



◆ CO2 (H₂/CO₂) ◇ acetate (H₂/CO₂)

Figure S1 individual plots of the isotopic value of the data shown in Fig 2. *S. sphaeroides* grown on different substrates (A = methanol, B = formate, C = H₂/CO₂).

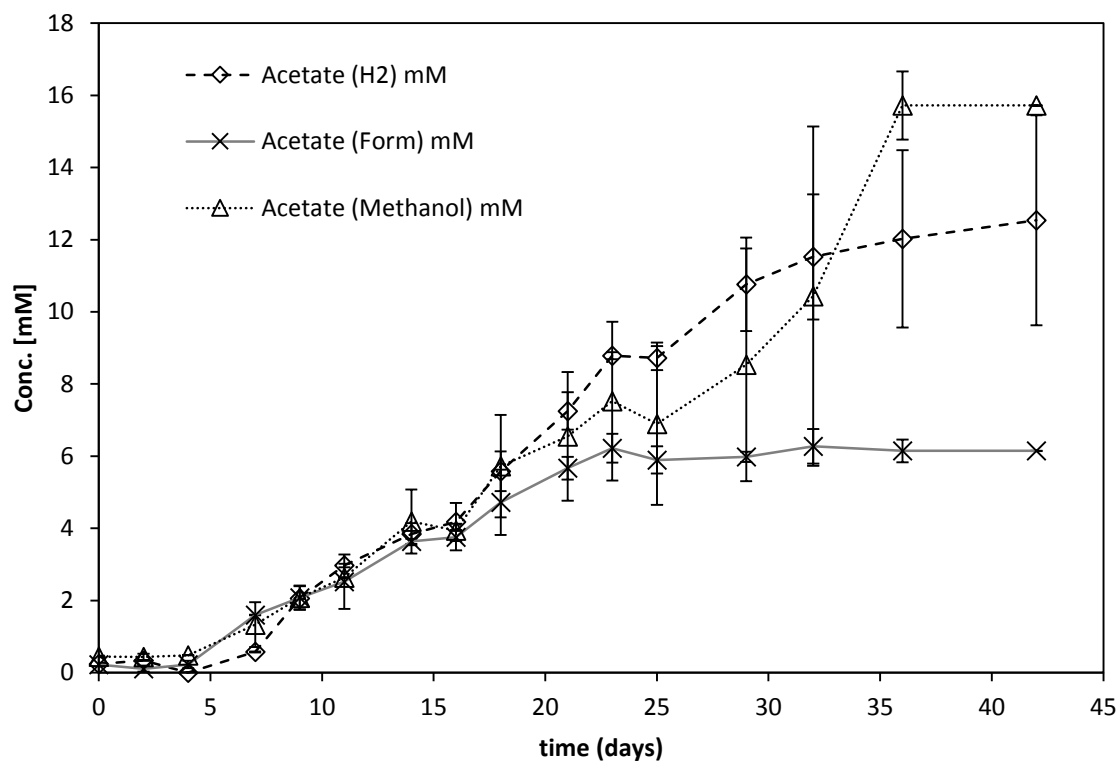


Figure S2 Acetate formation for *S. sphaeroides* grown on the expense of methanol (20mM) formate (20mM) or H₂/CO₂.

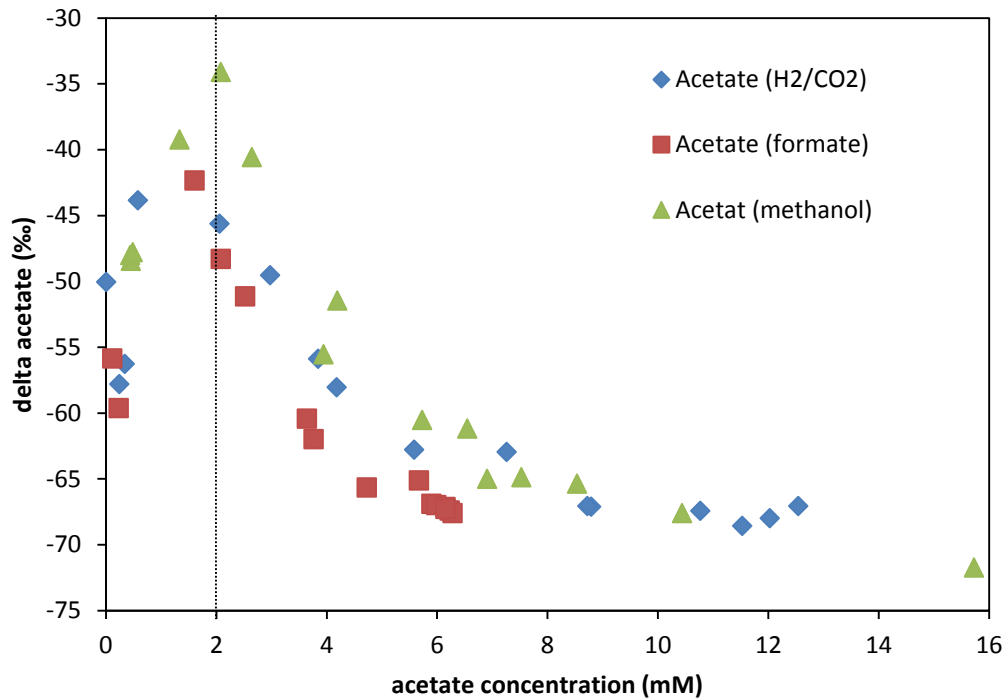


Figure S3 Acetate concentration vs. isotopic signal of acetate for *S. sphaeroides* grown on different substrates (compare Fig 2 for isotope values over time, Fig S2 for the individual isotope plots and Fig S3 for the acetate formation over time). While initially the delta ¹³C value of the acetate increases (until about day 10; compare Fig. 2) it later decrease to reach -65 to -70‰.

Discussion:

Usually an increase in the delta ¹³C of a compound origin in the consumption of this compound where the light isotopes are preferentially transferred to the product leaving the remaining substrate isotopically enriched. The depletion of the acetate delta ¹³C value could therefore be caused by a depletion of the acetate pool by either reverse acetogenesis (which so far has only been described for syntrophic associations) or cell growth on the expense of acetate. However, as can be seen in Fig. S7 the acetate values are roughly constant during the first five days of incubation and then linearly increase with a similar slope for all tested substrates. Hence a depletion of the acetate pool seems unlikely.

Alternatively a depletion of the acetate signal can be explained by an exchange reaction of the carboxyl-group of acetate with the carbonate / bicarbonate pool (1-4). The acetate concentrations are very low at that time (below 2mM = 100µmol) while the total inorganic carbon pool (bicarbonate

buffer 4.5 mmol + CO₂ in headspace 0.6 mmol) is relatively large. Such an exchange would therefore incorporate relatively heavy carbon (-17 to -18‰ for the headspace CO₂) with an isotopically more depleted carboxyl-group of the acetate and hence depleted the overall signal of the acetate while leaving the signal of the bicarbonate pool largely unchanged.

Similarly such an exchange reaction could help to explain the sharp decrease in the delta ¹³C value of format in the *T. kivui* incubations under mixotrophic conditions shown in Fig 3 between day 14 and day 16. At that time the formate concentration is very low (compare Fig S5). Again the sharp decrease in formate can either be explain be newly formed formate which has been fractionated from e.g. CO₂; or it could originate from an exchange reaction of the formate pool with the very light acetate pool. Since the formate concentration in all other incubations (all of which) under H₂/CO₂ never drops to such low values (Fig. S5) a similar effect may be masked.

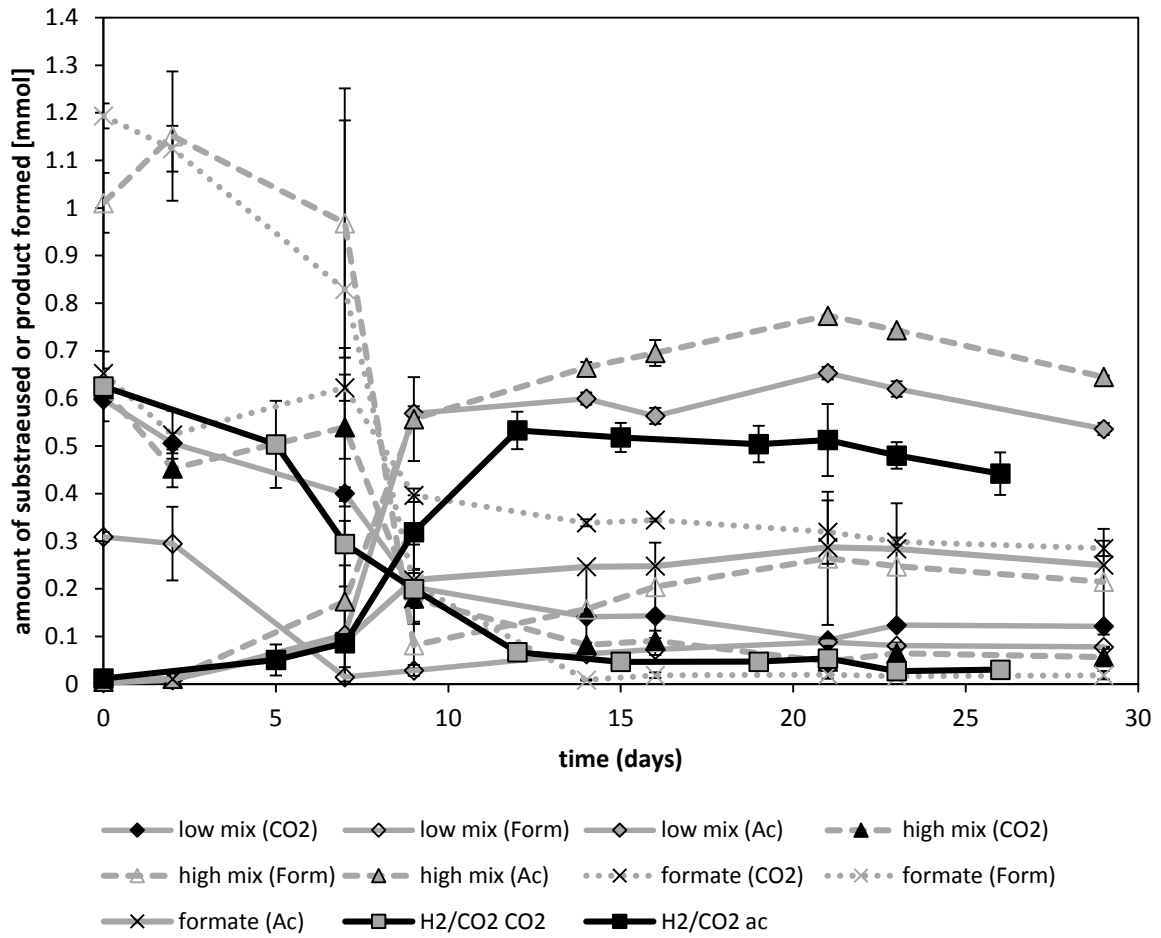


Figure S4 Substrate and product formation for *T. kivui* grown mixotrophically on different ratios of formate and H₂/CO₂.

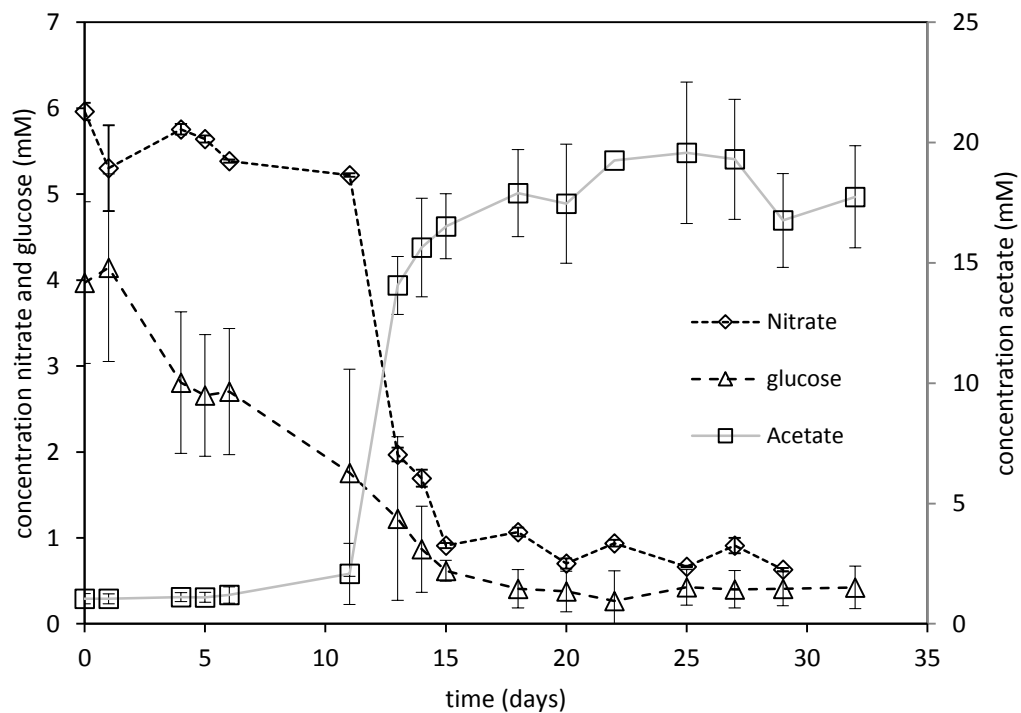


Figure S5. Concentration changes of substrate glucose, nitrate and the product acetate over time for *M. thermoacetica*. The concentration of nitrate was quantified using an HPLC-ion chromatography system. (n = 3; values given \pm SD)

***Thermoanaerobacter kivui* grown on glucose or H₂ / CO₂**

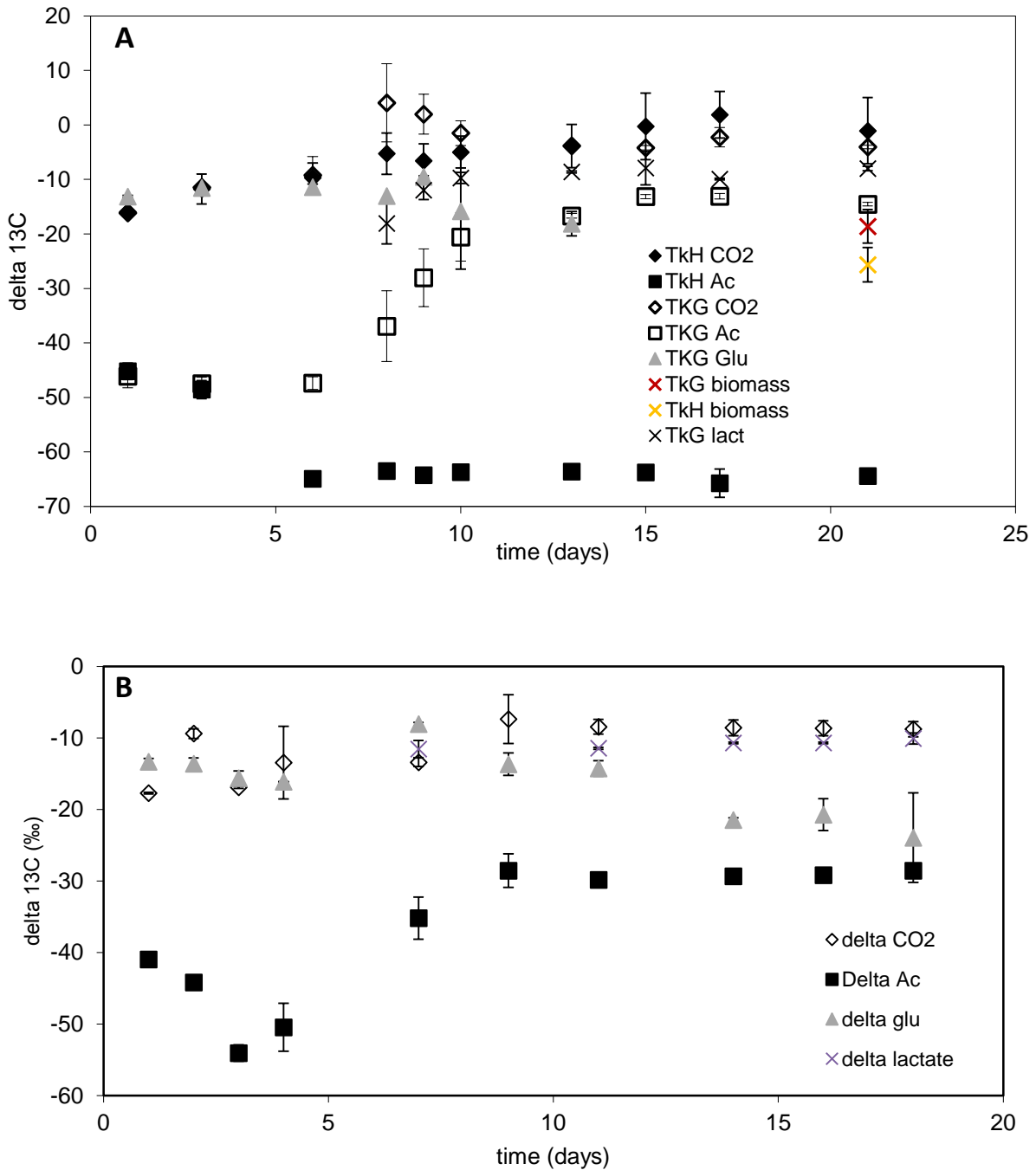


Figure S6. A: *T. kivui* grown on glucose TkG or H₂/CO₂ TkH. Depicted are the isotopic values of the glucose (Glu), CO₂, acetate and lactate (lact). The initial 52.4 mM glucose have been converted to 35.7 mM lactate and 81 mM acetate (89.7 % carbon recovery). The fractionation between CO₂ and acetate is $\epsilon_{\text{H}_2/\text{CO}_2} = -53.0 \text{ ‰}$ the fractionation between glucose and lactate was $\epsilon_{\text{Glu}} = -14.1 \text{ ‰}$. **B:** *T. kivui* grown on glucose in a phosphate buffered medium (The medium composition is largely the same but containing a phosphate buffer instead of the bicarbonate; compare Blaser *et al.* 2015 (5)). The initial 9.7 mM glucose have been converted to 6.5mM lactate and 15.4 mM acetate (carbon recovery 86.6 %) The fractionation between glucose and acetate was $\epsilon_{\text{Glu}} = -13.4 \text{ ‰}$.

Discussion:

It should be noted that the experimental conditions in the experiments shown in Fig S6 are different from the conditions during the fractionation into the biomass experiment depicted in Fig. 4. In the later experimental set up a lower glucose concentration (4mM) was used; no lactate was formed. In contrast to all other experiments having an initial glucose delta ^{13}C value of about $\epsilon_{\text{Glu}} = -14 \text{ ‰}$ the initial glucose isotope signal in the biomass experiment (Fig. 4) was around $\epsilon_{\text{Glu}} = -27 \text{ ‰}$. This may be one explanation why the fractionation factor for glucose into biomass as well as into acetate is unexpected low in this experiment. Indeed we would have expected an intermediate fractionation factor of -15 to -20 ‰ like we observed in Fig. 3 & Fig. S6. While part of the electrons for the data in Fig. 6 are directed to lactate formation due to the huge substrate excess, we indeed would expect an even slightly lower fractionation in the experimental data shown in Fig. 4.

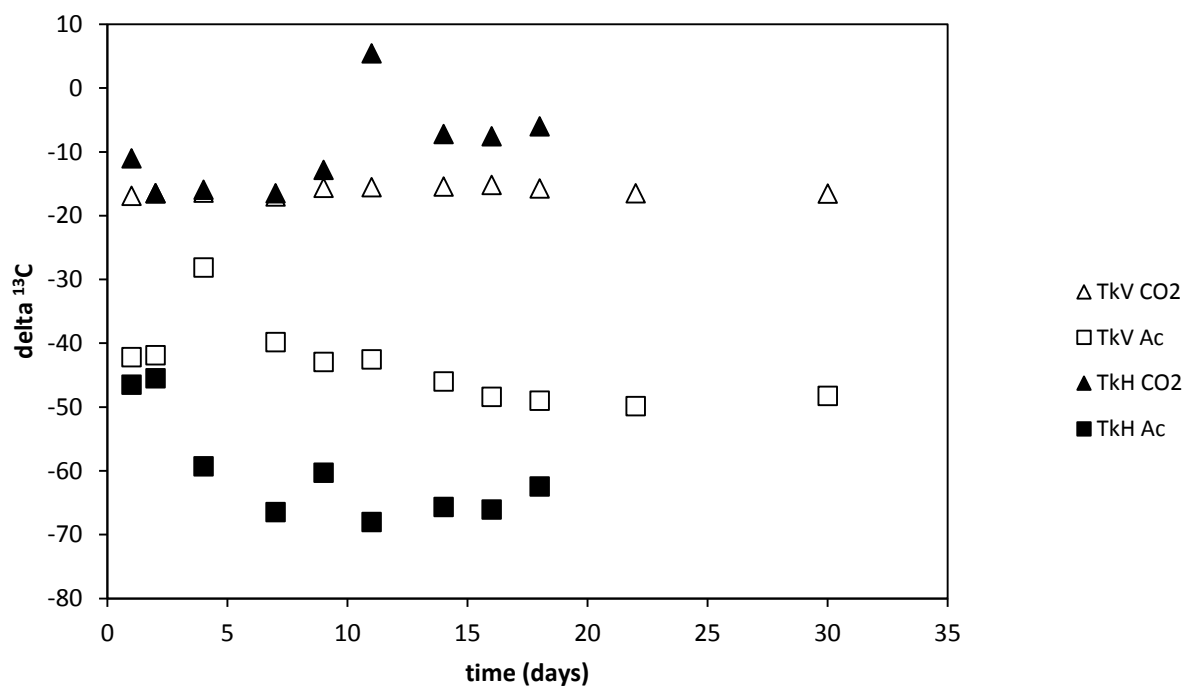


Figure S7. *Thermoanaerobacter kivui* growing on the expense of vanillic acid (TkV) or H₂/CO₂ (TkH). Shown is the isotopic signal of CO₂ (triangles) as well as acetate (squares). The isotopic signal of the vanillic acid could not be validated using our HPLC-IRMS approach. The initial $\delta^{13}\text{C}$ value of the vanillic acid was $\delta_{\text{van}} = -26.7 \text{ ‰}$.

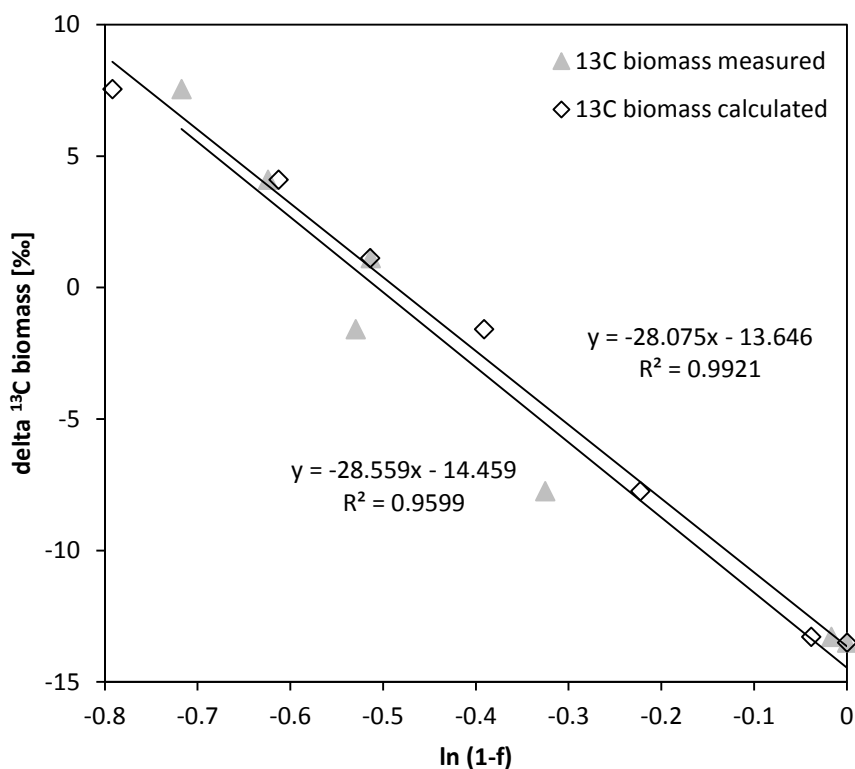


Figure S8. Comparison of the linear regression of the measured and calculated $\delta^{13}\text{C}$ values of the biomass. $\delta^{13}\text{C}$ values of the biomass were calculated assuming that the biomass is formed from pyruvate, which derives from carboxylation of acetate. Hence the $\delta^{13}\text{C}$ values of the biomass were calculated a simple mixing of the acetate signal (2/3) and the CO_2 of the headspace (1/3) for each measured time point. If the biomass would primarily stem directly from acetyl-CoA (e.g. fatty acids) the resulting isotopic signal would be expected to correspond to the original acetyl-CoA signal shown in Fig 4.

Discussion:

In order to generate bulk biomass, acetyl-CoA can either serve directly as building block to synthesize e.g. fatty acids or it can be carboxylated to pyruvate which then serves as the building block for e.g. amino acid synthesis. In the first case the isotopic signal of the biomass would resemble the $\delta^{13}\text{C}$ depleted acetyl-CoA. In contrast carboxylation to pyruvate may incorporate heavier CO_2 resembling the $\delta^{13}\text{C}$ value of the CO_2 in the headspace (or the total inorganic carbon) rendering an isotopic signal of the bulk biomass which is a mixed signal of the acetate (2/3) and CO_2 (1/3) ^{13}C values (**Fig. S8**). Assuming the second scenario a similar calculation can be performed for the data given in Londry *et al.* (6) for hydrogenotrophic methanogenesis yielding an isotope signal for the biomass of -44.6 ‰

(calculated) vs -45.1‰ (measured). It is however intriguing to note that the fractionation into biomass for *T. kivui* grown on glucose is likewise roughly $2/3$ of the fractionation into acetate. However the absolute values ($\epsilon_{\text{catabol.}} = +4.2\text{‰}$; $\epsilon_{\text{anabol.}} = +2.9\text{‰}$) are quite similar and may not have any implications for environmental studies. Indeed one would assume that the biomass ($\delta_{\text{biomass}} = -27.3 \pm 1.9\text{‰}$) under these conditions stems from pyruvate formed during glycolysis and hence should have a similar isotope signal as the original glucose $\delta_{\text{glu}} = -27.9 \pm 0.9\text{‰}$.

SCFA determination using HPLC-IRMS

In previous publications we used a separate HPLC system operated under the similar conditions as the HPLC-IRMS to quantify the concentrations of SCFA and Glucose: We used the same eluent (1mM H₂SO₄ at 0.5ml/min) the same ion-exclusion column (Aminex HPX-87-H, BioRad, München, Germany) and run an UV-Detector (Sykam, Germany) as well as a Refraction Index detector. Data analysis was done using the Clarity Software package. This system provides a high sensitivity and due to the two detectors a high accuracy. The linear correlation usually covered the observed substrate / product concentrations of up to 20 mM and proved to have a high precision down to several µM. For the isotope analysis the samples were usually diluted to have proximally 0.5 to 5 mM SCFA and analysed on the HPLC-IRMS system as described in the main manuscript. As can be exemplarily seen for acetate in Fig. S4 the HPLC-IRMS signal gives a linear response in this concentration range. Therefore, we directly used the HPLC-IRMS to quantify the concentration of SCFA in pure culture experiments. In this range the isotopic signal of acetate was -42.7 ± 0.3 ‰ irrespective of the acetate concentration. Repeated injections (n=10) of 1mM acetate gave an area of 397.8 ± 4.3 Vs. At higher concentrations the oxidation reaction of acetate to CO₂ is not complete, which is usually directly seen in the broadened peak shape of the Chromatogram.

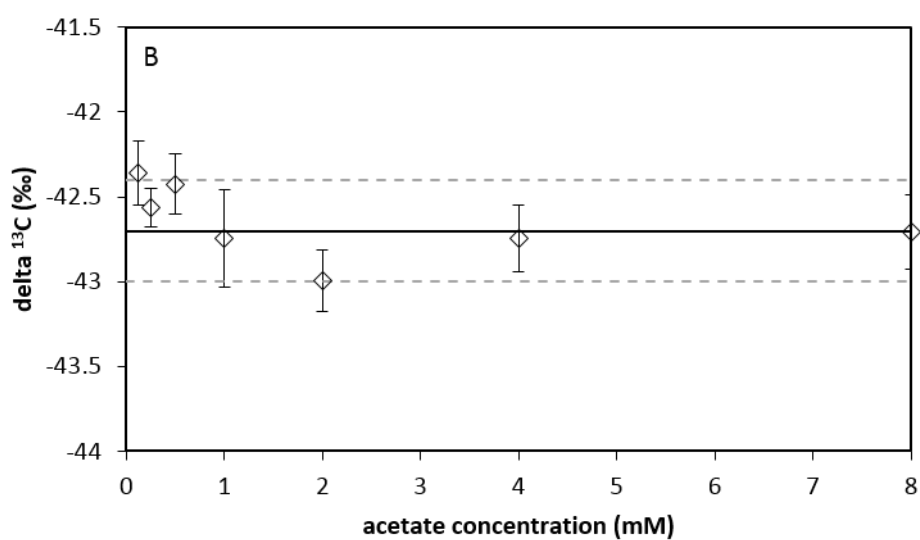
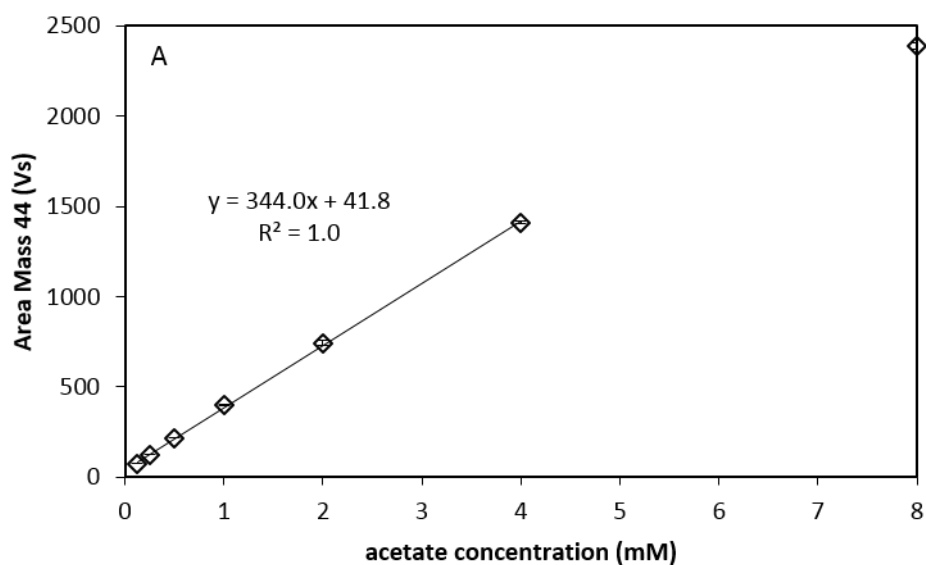


Figure S9 **A)** Acetate concentration determined by the HPLC-IRMS ($n = 3 \pm \text{SD}$). **B)** isotopic signature of the respective acetate samples ($n = 3 \pm \text{SD}$). The average of all samples (-42.7‰) is given as black line; the standard deviation ($\pm 0.7 \text{‰}$) as broken line.

Table S2 HPLC-IRMS results for different SCFA and glucose.

Analyte	Retention time (min)	Area 44 (Vs) of a 1mM solution	Delta 13C (‰)
Glucose	12.1	1287.8	-12.7
Formate	17.6	246.2	-24.8
Acetate	19.2	397.8	-42.7
Methanol	23.9	798.7	-29.8

References

1. **Eikmanns B, Thauer RK.** 1984. Catalysis of an isotopic exchange between CO₂ and the carboxyl group of acetate by *Methanosarcina barkeri* grown on acetate. *Archives of Microbiology* **138**:365-370.
2. **Fischer R, Thauer RK.** 1990. Methanogenesis from acetate in cell-extracts of *Methanosarcina barkeri* - isotope exchange between CO₂ and the carbonyl group of acetyl-CoA, and the role of H₂. *Archives of Microbiology* **153**:156-162.
3. **Raybuck SA, Ramer SE, Abbanat DR, Peters JW, Ormejohnson WH, Ferry JG, Walsh CT.** 1991. Demonstration of carbon-carbon bond-cleavage of acetyl coenzyme-A by using isotopic exchange catalyzed by the CO dehydrogenase complex from acetate-grown *Methanosarcina thermophila*. *Journal of Bacteriology* **173**:929-932.
4. **Spormann AM, Thauer RK.** 1989. Anaerobic acetate oxidation to CO₂ by *Desulfotomaculum acetoxidans* - isotopic exchange between CO₂ and the carbonyl group of acetyl-CoA and topology of enzymes involved. *Archives of Microbiology* **152**:189-195.
5. **Blaser MB, Dreisbach LK, Conrad R.** 2015. Carbon isotope fractionation of *Thermoanaerobacter kivui* in different growth media and at different total inorganic carbon concentration. *Organic Geochemistry* **81**:45-52.
6. **Londry KL, Dawson KG, Grover HD, Summons RE, Bradley AS.** 2008. Stable carbon isotope fractionation between substrates and products of *Methanosarcina barkeri*. *Organic Geochemistry* **39**:608-621.

7. **Goevert D, Conrad R.** 2008. Carbon isotope fractionation by sulfate-reducing bacteria using different pathways for the oxidation of acetate. *Environmental Science & Technology* **42**:7813-7817.
8. **Goevert D, Conrad R.** 2009. Effect of substrate concentration on carbon isotope fractionation during acetoclastic methanogenesis by *Methanosarcina barkeri* and *M. acetivorans* and in rice field soil. *Applied and Environmental Microbiology* **75**:2605-2612.
9. **House CH, Schopf JW, Stetter KO.** 2003. Carbon isotopic fractionation by Archaeans and other thermophilic prokaryotes. *Organic Geochemistry* **34**:345-356.
10. **Penger J, Conrad R, Blaser M.** 2012. Stable Carbon Isotope Fractionation by Methylophilic Methanogenic Archaea. *Applied and Environmental Microbiology* **78**:7596-7602.
11. **Preuss A, Schauder R, Fuchs G, Stichler W.** 1989. Carbon isotope fractionation by autotrophic bacteria with 3 different CO₂ fixation pathways. *Zeitschrift fur Naturforschung C-A Journal of Biosciences* **44**:397-402.
12. **Zhang CLL, Ye Q, Reysenbach AL, Gotz D, Peacock A, White DC, Horita J, Cole DR, Fong J, Pratt L, Fang JS, Huang YS.** 2002. Carbon isotopic fractionations associated with thermophilic bacteria *Thermotoga maritima* and *Persephonella marina*. *Environmental Microbiology* **4**:58-64.
13. **Zyakun AM, Kochetkov VV, Baskunov BP, Zakharchenko VN, Peshenko VP, Laurinavichius KS, Anokhina TO, Siunova TV, Sizova OI, Boronin AM.** 2013. Use

of glucose and carbon isotope fractionation by microbial cells immobilized on solid-phase surface. *Microbiology* **82**:280-289.

14. **Zyakun AM, Lunina ON, Prusakova TS, Pimenov NV, Ivanov MV.** 2009.

Fractionation of stable carbon isotopes by photoautotrophically growing anoxygenic purple and green sulfur bacteria. *Microbiology* **78**:757-768.